EUROPHYSICS LETTERS 1 April 1998

Europhys. Lett., **42** (1), pp. 91-96 (1998)

Magnetic properties of Ni nanoparticles dispersed in silica prepared by high-energy ball milling

E. M. González[1](*), M. I. Montero[1], F. Cebollada[1], C. de Julián[1]
J. L. Vicent[2] and J. M. González[2]

[1] *Instituto de Ciencia de Materiales de Madrid-CSIC*
28049 Cantoblanco, Madrid, Spain
[2] *Departamento de Física de Materiales, Facultad de Ciencias Físicas*
Universidad Complutense - Avda. Complutense s/n 28040 Madrid, Spain

(received 7 November 1997; accepted in final form 9 February 1998)

PACS. 75.50Tt – Fine-particle systems.
PACS. 75.40Cx – Static properties (order parameter, static susceptibility, heat capacities, critical exponents, etc.).
PACS. 75.60Nt – Magnetic annealing and temperature-hysteresis effects.

Abstract. – We analyze the magnetic properties of mechanically ground nanosized Ni particles dispersed in a SiO_2 matrix. Our magnetic characterization of the as-milled samples show the occurrence of two blocking processes and that of non-monotonic milling time evolutions of the magnetic-order temperature, the high-field magnetization and the saturation coercivity. The measured coercivities exhibit giant values and a uniaxial-type temperature dependence. Thermal treatment carried out in the as-prepared samples result in a remarkable coercivity reduction and in an increase of the high-field magnetization. We conclude, on the basis of the consideration of a core (pure Ni) and shell (Ni-Si inhomogeneous alloy) particle structure, that the magnetoelastic anisotropy plays the dominant role in determining the magnetic properties of our particles.

Introduction. – The size reduction, down to the nm scale, of the structural correlation length characterizing magnetic systems has a number of consequences both on their structure-dependent properties and on their hysteretic behaviour [1]. Examples of this are the modifications of the magnon spectrum [2] and the relevant role on the global behaviour of the nanoentities of the "surface" (actual particle surface structures or grain boundaries) values of the magnetic moments, exchange interactions, order temperature and anisotropy [3]. From the point of view of the hysteretic properties, the reduction of the structural correlation length below the magnetic correlation one results either in extremely soft behaviours (induced by the averaging of the local properties) if the nanoentities are coupled through exchange and/or dipolar interactions or in giant coercivities if demagnetize in a non-collective way [4]. Magnetic nanoparticles have been prepared by means of different techniques including physical vapour deposition ones, chemical methods and mechanical grinding [5]. The interest of this last technique is linked to the possibility of easily achieving extreme size reductions [6], to its potential for the preparation of large amounts of material and to its economic implementation.

Preparation of samples and experimental techniques. – We have prepared nanoparticulate samples with nominal composition given by $Ni_x/(SiO2)_{1-x}$, where x denoted the Ni volume

(*) E-mail:immgf4a@fresno.csic.es

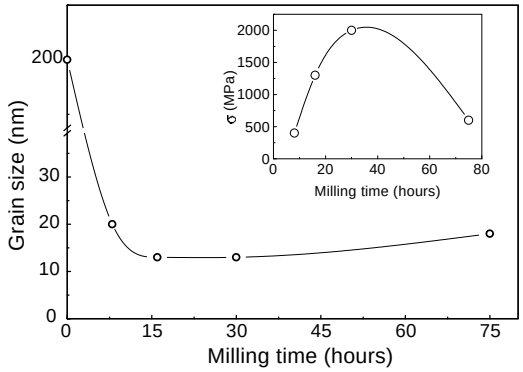

Fig. 1. – Milling time dependence of the average grain size for the $x = 0.3$ samples. The inset shows the milling time dependence of the residual stresses present in this sample.

fraction and ranged from 0.1 up to 0.4. The samples were prepared by high-energy ball milling starting from a mixture of -325 mesh Ni powders and amorphous SiO_2 gel. That mixture was sealed under Ar in a hardened stainless-steel jar together with balls of the same material. The powder-to-balls mass ratio was of 1:14. The mixture was milled for times of up to 75 hours. The microstructural characterization of the samples involved X-ray diffraction (XRD) and transmission electron microscopy (TEM). The Curie temperature of the samples was measured at zero applied field by using a differential scanning calorimeter (DSC) unit. The magnetic properties study was performed in the temperature range going from 1.7 up to 300 K by using vibrating sample and SQUID magnetometers.

Results and discussion. – X-ray diffractograms taken in the as-milled samples showed the presence of Ni reflections without any trace of oxidation. Figure 1 shows the evolution with the milling time of the average grain size as evaluated from the Ni (111) reflections by using the Scherrer formula [7]. The average grain size exhibited a non-monotonic evolution characterized by the occurrence of a minimum for milling times in the range from 15 to 30 hours. Measurement of the (111) reflection displacement allowed us to estimate (considering a Ni Young modulus of 200 GPa [8]) the milling time dependence of the average residual stresses. Our data, shown in the inset in fig. 1 evidence stress levels reaching the GPa order.

The TEM observations (see fig. 2) revealed a broad distribution of particle sizes (see the inset in fig. 2) and the occurrence of some degree of particle clustering. From the analysis of the TEM images we concluded that the average particle size coincided with the average grain size in the milling time range corresponding to the minimum in fig. 1. For longer milling times the average particle size increased more rapidly than the average grain size. This evolution of the morphologic and structural parameters reflects the compromise between the two elemental mechanisms taking place during milling: particle fracture (originated by the different mechanical properties of Ni and SiO_2) and particle welding (produced through collisions between the metallic particles).

In fig. 3a) we have plotted our results for the milling time dependence of the Curie temperature of the $x = 0.3$ and $x = 0.4$ samples. Correlation of these results with those corresponding to the average grain and particle size dependences on the milling time, evidenced that the order temperature markedly decreased with the average grain size in the milling time range in which the average grain and particle sizes coincided. After a minimum (corresponding, in the case of the $x = 0.3$ sample, to a T_c decrease of 7% with respect to the bulk material value) we observed an increase of the order temperature up to its bulk value which was clearly related to the increase of the average particle size. A typical example of the temperature dependence of

Fig. 2. – TEM image of the nanostructure present in the $x = 0.3$, 16 hours milled sample. The inset shows the associated particle size distribution.

the low-field (5.0×10^{-3} T) magnetic moment of the samples is shown in fig. 3b). It corresponds to the $x = 0.3$, 30 hours milled sample. Figure 3b) presents data, obtained after zero-field cooling (ZFC) and field-cooling (FC, 5.0×10^{-3} T) the sample and evidences i) the occurrence of a low-temperature (ca. 5 K) blocking process (see the inset in fig. 3b) and ii) that of a high-temperature one (corresponding to a blocking temperature above 300 K).

In fig. 4a) we present the milling time dependence of the high-field (1 T) magnetization measured, at room temperature, in the as-milled samples. In all the cases, the magnetization initially decreased with the increase of the milling time (as more and more particles got superparamagnetic with the milling time induced reduction of the particle size). For longer milling times, *i.e.* in the milling time range in which the compromise between particle fracture and particle welding originated polycrystalline aggregates, a tendency to the increase of the high-field magnetization was observed. The coercive force of all the studied samples was measured at room temperature after applying a field of 2.5 T (see fig. 4b). Our coercive force results are again correlated with the milling time evolution of the particle size. The coercive force increased (up to giant values, in the sense that they were not compatible with

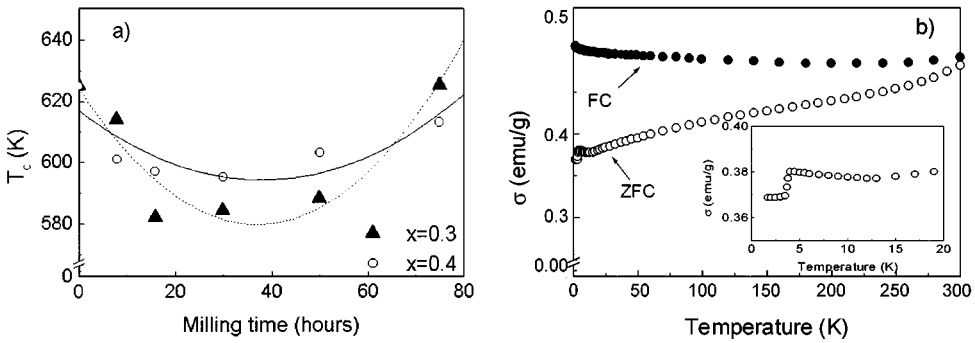

Fig. 3. – a) Milling time dependence of the Curie temperature measured in the $x = 0.3$ and $x = 0.4$ samples. b) Field-cooling and zero-field-cooling curves measured in the $x = 0.3$, 30 hours milled sample.

the bulk value of the Ni magnetocrystalline anisotropy constants) in the milling time range in which particle size decreased, reaching a maximum for milling times similar to those for which a minimum particle size was observed. For longer milling times, coercivity decreased to Ni bulk-like values.

The temperature dependence of the coercive force measured in the $x = 0.4$, 8 hours milled sample is shown in fig. 5, where it is apparent that our data closely follow a $T^{0.77}$ law corresponding to an isotropic distribution of non-interacting, uniaxial [9]. We have also investigated the effect of the stress relaxation treatments on both the magnetization and the coercive-force values. The as-milled samples were thermally treated by continuously heating them, at a rate of 80 K min^{-1}, from room temperature up to 775 K and keeping them at this temperature for times in the range from 0 up to 25 minutes (after the treatment they were cooled down to room temperature at a rate of 200 K min^{-1}). The treatments were carried out in a DSC unit. X-ray diffractograms obtained in the treated samples evidenced the occurrence of grain growth: for instance, in the samples milled for 75 hours the average grain size increased up to 50 nm after the relaxation anneal.

In fig. 6a) we present the milling time dependence of the magnetization (measured under an applied field of 1 T) of the treated $x = 0.3$ samples. The increase of the magnetization with the thermal treatment brought the magnetization of all the samples to values close to that

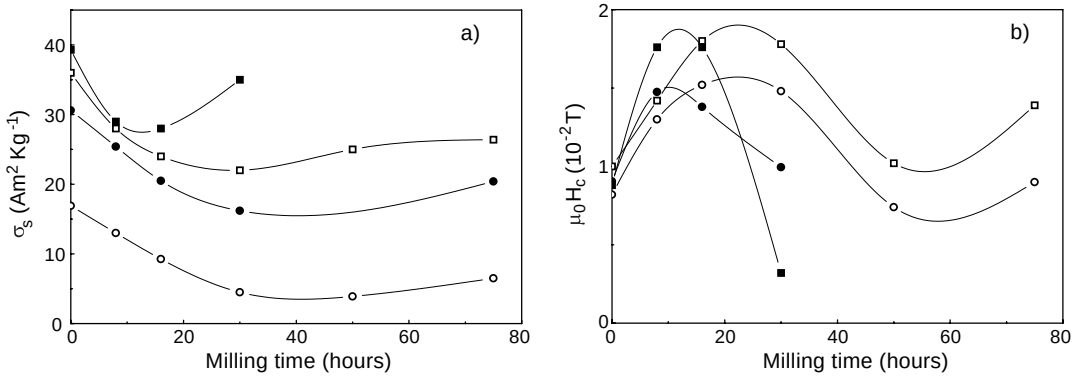

Fig. 4. – Milling time dependence of a) the magnetization measured under an applied field of 1 T and b) the saturation coercive force (as-milled samples, ■ $x = 0.4$, □ $x = 0.3$, ● $x = 0.2$, ○ $x = 0.1$).

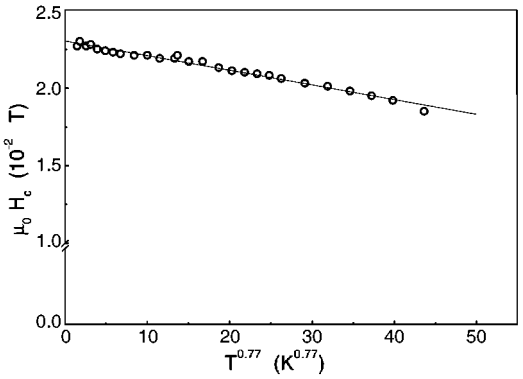

Fig. 5. – Temperature dependence of the saturation coercivity ($x = 0.2$, 8 hours milled sample).

corresponding to the unmilled sample. The results corresponding to the coercivity of these samples, presented in fig. 6b), show a large coercivity reduction.

Discussion and conclusion. – Our results for the Curie temperature dependence on the milling time show a reduction of that quantity having the same magnitude than that reported in [10] for nanocomposite Ni/Al_2O_3 thin films having particle sizes in the range from 2 to 5 nm. We should point out that, similarly to the case of the Fe/SiO_2 mechanically ground samples in which an amorphous Fe-Si surface layer was detected by using Mössbauer spectroscopy [11], we cannot exclude the occurrence of some degree of Ni-Si alloying. By considering a core (pure Ni) and shell (inhomogeneous Ni-Si alloy) model for our particles (those present in the samples milled for times shorter than 30 hours), and remembering the rapid decrease of the Curie temperature associated to the dilution of Si in Ni (T_c of the solid solution goes down to 300 K for a 6% at. Si [12]) we can relate the observed T_c decrease to an effective particle volume (that of the core) lower than that observed through XRD and TEM.

In the case of the samples milled for times longer than 30 hours (polycrystalline particles) the welding process resulting in the increase of the average particle size leads to a T_c increase which could be ascribed to either (grain) core interactions or to the elimination upon grain aggregation of the shell layer. The core and shell model can also be related to the occurrence (detected in the ZFC and FC curves) of two blocking processes. Regarding that taking place

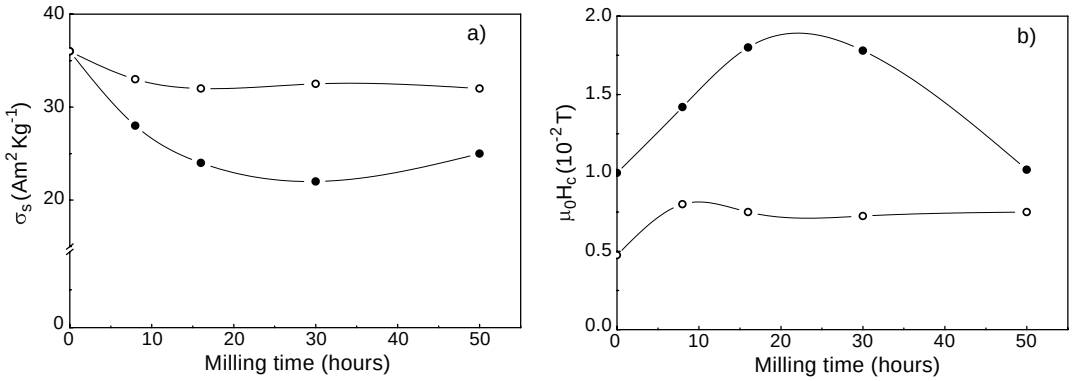

Fig. 6. – Milling time dependence of a) the magnetization measured under an applied field of 1 T and b) the saturation coercive force, measured in the $x = 0.3$ samples (● as-prepared and ○ treated at 775 K).

at temperatures above 300 K (which we identify with the particle core), we should point out that it cannot be related to the Ni magnetocrystalline anisotropy even considering an effective particle volume equal to that measured by XRD and TEM (the blocking temperature corresponding to a Ni particle having a diameter of 15 nm and cubic anisotropy constants of $K_{1\mathrm{Ni}} = -5.5 \times 10^3$ Jm^{-3} and $K_{2\mathrm{Ni}} = -2.5 \times 10^3$ Jm^{-3}, is 170 K). This suggests the existence of an additional contribution to the effective anisotropy which could be related either to magnetoelastic interactions or to the particle shape.

Our TEM observations, did not reveal any indication of large particle anisometry which allows us to rule out a significant contribution to the effective anisotropy of the shape anisotropy. Differently from this, the magnetoleastic anisotropy can go clearly beyond the magnetocrystalline anisotropy values: if we consider a magnetostriction constant λ_{S} similar to that of the bulk Ni, $\lambda_{\mathrm{S}} = 5 \times 10^{-5}$, and the residual stress, σ, levels resulting from our XRD experiments (see fig. 1), the order magnitude of the magnetoelastic anisotropy constant, $K_{\mathrm{mel}} = (3/2)\lambda_{\mathrm{S}}\sigma$, could be as high as $K_{\mathrm{mel}} = 1.5 \times 10^5$ Jm^{-3}.

As for the low-temperature blocking process, we propose that it should be related to the particle shell. The presence in this shell region of Si diffusion into the Ni lattice should significantly reduce the local anisotropy [12] which could explain the large blocking temperature difference with the particle core. Our coercivity data and, more concretely, the occurrence of giant coercivities and their temperature dependence, showing a good agreement with the $T^{0.77}$ law, confirm that the magnetization reversal of our particles is not ruled by the Ni magnetocrystalline anisotropy. Let us remember in this sense the fact that Ni exhibits cubic anisotropy which is not compatible with the $T^{0.77}$ behaviour, characterizing uniaxial particles.

Nevertheless, large magnetoelastic anisotropies can make a cubic crystal to behave as a uniaxial one which supports our hypothesis about the dominant role of the magnetoleastic anisotropy on the magnetic properties of the particles. This is also supported by the observed decrease of the coercivity induced by stress relaxation-type thermal treatments.

Finally, the observed increase of the high-field magnetization induced by the thermal treatments could be related to a combination of magnetoelastic anisotropy relaxation and of chemical rearrangements on the grain/particle shell region resulting on the growth of the core volume.

REFERENCES

[1] Abeles B., Sheng P., Couts N. D. and Aries Y., *Adv. Phys.*, **24** (1975) 407.
[2] García N., in *Science and Technology of Nanostructured Magnetic Materials*, edited by G. C. Hadjipanayis and G. A. Prinz (Plenum Press, New York) 1991, p. 581.
[3] Gradmann U., in *Ferromagnetic Materials: Handbook of Magnetic Materials*, edited by K. H. J. Buschow, Vol. 7 (Elsevier, London) 1993, p. 1.
[4] Herzer G., *IEEE Trans. Magn.*, **25** (1989) 3327.
[5] Chien C. L., in *Science and Technology of Nanostructured Magnetic Materials*, edited by G. C. Hadjipanayis and G. A. Prinz (Plenum Press, New York) 1991, p. 477.
[6] Giri A. K., de Julián C. and González J. M., *J. Appl. Phys.*, **76** (1994) 6573.
[7] Klug H. P. and Alexander L. E., in *X-ray Diffraction Procedures for Polycrystalline and Amorphous Materials* (John Wiley and Sons, New York) 1974, p. 687.
[8] *CRC Handbook of Chemistry and Physics* (CRC Press, Boca Raton) 1995, pp. 12-185.
[9] Pfeiffer H., *Phys. Stat. Solidi A*, **120** (1990) 233.
[10] Gavrin A. and Chien C. L., *J. Appl. Phys.*, **73** (1993) 6949.
[11] de Julián C., Pérez Alcázar G. A., González J. M. and Marco J. F., submitted to *J. Appl. Phys.*
[12] Marian V., *Ann. Phys.* (*Paris*), **7** (1937) 459.